*Journal of Engineering Physics and Thermophysics, Vol. 71, No. 6, 1998*

# POSSIBILITY OF METHANE DECOMPOSITION IN A GAS DISCHARGE

O. V. Petrova, P. I. Porshnev, and
S. A. Zhdanok

UDC 533.92

*The possibility of using a gas discharge such as a corona discharge or a barrier discharge for decomposition of methane in different gaseous mixtures is investigated theoretically. The effect of preheating of the gas to a temperature of 1200 K on the degree of methane conversion in the discharge is studied. A kinetic model that describes the processes of methane decomposition and oxidation in* $CH_4/CO_2$*,* $CH_4/H_2O$*, and* $CH_4/O_2$ *mixtures is developed. The effect of the discharge parameters and gas additives on the efficiency of methane decomposition is investigated. The optimum temperature of the mixture, particle lifetime, and initial concentration of oxygen for the production of hydrogen molecules are found.*

Chemical transformations of hydrocarbons are of great practical interest for fine organic synthesis, for processes of formation of polymer films and protective coatings, and as the most inexpensive method for producing carbon and $H_2$ (see, for example, [1-3]). The products of the decomposition of mixtures of methane with carbon dioxide, water, or air are widely used for catalytic synthesis of hydrocarbon mixtures and other chemical products. The traditional technology of hydrocarbon decomposition, based on thermal cracking or catalytic methods, is characterized by low degrees of conversion and high energy consumption. In this connection, the development of new methods that use a low-temperature plasma is of greatest interest. It is known that a methane molecule is very stable with a dissociation energy of the order of 9 eV, and therefore methane is decomposed at very high temperatures, characteristic of an arc discharge [4-6]. We investigate the possibility of using low-temperature gas discharges such as a corona discharge or a barrier discharge for efficient dissociation of methane molecules and their transformation to molecules with a higher content of carbon and hydrogen such as $C_2H_6$, $C_2H_5$, $C_2H_4$, and others. Thermal dissociation of the latter occurs at lower temperatures than methane dissociation and, consequently, mutual account of the processes of methane dissociation in a gas discharge and thermal decomposition of intermediate products due to preheating of the gas will lead to a substantial increase in conversion of methane under conditions where the thermal dissociation of methane is insignificant. A decrease in the energy consumption required for such high-energy processes as transformation of methane to hydrogen, acetylene, ethylene, etc. is possible here.

In the past decade, numerous plasmachemical investigations of hydrocarbon decomposition in a nonequilibrium plasma have been performed. However, the main portion of these works were performed in low-pressure discharges such as glow, high-frequency, and microwave discharges. In this work, we studied methane decomposition in atmospheric-pressure discharges. A corona discharge, distinguished by simplicity of implementation, insignificant energy consumption, and high efficiency of stimulation of the chemical processes, occupies a special place among them. Owing to this it is widely used in industry, for example, for removing nitrogen and sulfur oxides from gas releases [7]. It is known that in a corona discharge the main portion of the electron energy enters into the electronic degrees of freedom of the gas molecules rather than the vibrational degrees of freedom, as is the case in a glow discharge (which leads to additional heating of the gas). Therefore the processes of dissociation of methane molecules and thermal heating of a gaseous mixture can be considered independently of one another in a corona discharge. Below we study the kinetics of methane decomposition in a preheated gas discharge and determine the optimum mechanisms of occurrence of this process.

---

Academic Scientific Complex "A. V. Luikov Institute of Heat and Mass Transfer of the National Academy of Sciences of Belarus," Minsk, Belarus. Translated from Inzhenerno-Fizicheskii Zhurnal, Vol. 71, No. 6, pp. 1016-1023, November-December, 1998. Original article submitted May 12, 1998.

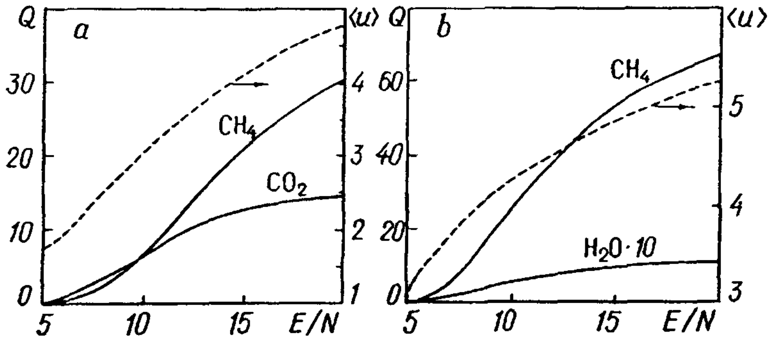

Fig. 1. Fractions of the energy expended on dissociation and average electron energies as functions of the reduced electric field in the mixtures: a) $CH_4/CO_2 = 50{:}50$; b) $CH_4/H_2O = 95{:}5$. $Q$, %; $\langle u \rangle$, eV; $E/N$, $10^{-16}$ V·cm$^2$.

The initial step of $CH_4$ conversion in a gas discharge is electron-impact dissociation of neutral molecules of the initial gaseous mixture. This reaction produces H, O, and $CH_3$ radicals, which interact actively with gas molecules. It is known that the rate constants for the reactions of molecules with electrons depend on the electron energy, which can be determined from the relation between the energy obtained from the electric field and the losses in elastic and inelastic collisions with the gas molecules. The electron-energy distribution in methane-containing mixtures was calculated by solving the solution of the Boltzmann equation by the method of binomial expansion [8]. The cross sections of electron collisions with gas molecules used in the calculations were taken from [9-12]. A total of 71 inelastic processes were allowed for in the work. A detailed description of the procedure of solving the Boltzmann equation is given in [13, 14]. As a result of the solution we calculated the electron energy distribution functions for each gaseous mixture and determined the fractions of the energy that go to dissociation of mixture molecules by electron impact as functions of the local electric field.

The fractions of the energy expended on dissociation, calculated for two gaseous mixtures, are presented in Fig. 1. As the calculations show, the contribution of the dissociation increases with the reduced electric field and becomes governing for $E/N$ that exceed $10^{-15}$ V·cm$^2$. For smaller reduced electric fields, the main portion of the electron energy goes to excitation of vibrational degrees of freedom of $CH_4$ and $CO_2$ molecules, which induces an increase in the gas temperature due to processes of vibrational-translational relaxation. The value $E/N = 10^{-15}$ V·cm$^2$ corresponds to an electric-field strength of 24.7 kV/cm at atmospheric pressure. In our calculations, we used $E/N = (1.5-2.0) \cdot 10^{-15}$ V·cm$^2$, for which the electron energy enters predominantly into dissociation channels. A more accurate evaluation of the reduced field for our conditions must allow for the model of streamer propagation, which is assumed to be done in what follows. Performing this analysis, we could show that, under the conditions in question, about 40-65% of the electric-field energy is expended on dissociation of molecules of the gaseous mixture by electron impact. This significant contribution to the dissociation is explained by the high average electron energies in the considered electric fields, comparable with the threshold values of the dissociation of $CH_4$, $CO_2$, and $H_2O$ molecules (the dashed lines in Fig. 1). As can be seen from the energy distribution over the various channels of dissociation it is methane dissociation that is governing, not only for the mixtures of methane and carbon dioxide or water (Fig. 1) but also for the mixture $CH_4/CO_2$/air = 40:40:20. The rate constants for the reactions of electron-impact dissociation $k^{\mathrm{diss}}$ are determined in solving the Boltzmann equation; however, within the framework of this approximation, it seems impossible to calculate local concentrations of electrons. They can be obtained with allowance for the model of streamer propagation, which is due to the unsteady and inhomogeneous nature of the discharge. In our calculations, we used the average dissociation frequency $\nu^{\mathrm{diss}} = \langle k^{\mathrm{diss}} \cdot N_e \rangle$, where $\langle\ \rangle$ denotes averaging over time and the spatial coordinate, with adoption of typical energies of the electric field, lifetimes, and flow rates of the gas measured in a corona discharge or a barrier discharge [15]. The estimated dissociation frequency, under our conditions, is $(4-7) \cdot 10^{-3}$ sec. The electron-impact dissociation of gas molecules is represented by reaction 21 in Table 1. This reaction can be considered to be a unimolecular process of decay of a molecule (AB) with a frequency proportional to the energy of the electric field. The possibility of adopting this approximation is associated with special features of the propagation of a streamer microchannel. It is known that

TABLE 1. Kinetic Mechanism of Decomposition and Oxidation of Methane

| No. of reaction | Reaction | *A* | *n* | *E*a | Literature source |
|---|---|---|---|---|---|
| 1 | $CH_4+H = CH_3+H_2$ | $1.33 \cdot 10^{4}$ | 3.0 | 8038 | [21] |
| 2 | $CH_4+OH = CH_3+H_2O$ | $1.57 \cdot 10^{7}$ | 1.83 | 2782 | [22] |
| 3 | $CH_4+O = CH_3+OH$ | $6.92 \cdot 10^{8}$ | 1.56 | 8485 | [22] |
| 4 | $CH_4+M = CH_3+H+M$ | $4.50 \cdot 10^{17}$ | 0.0 | 90,820 | [23] |
| 5 | $CO+OH = CO_2+H$ | $6.30 \cdot 10^{6}$ | 1.50 | −495 | [24] |
| 6 | $2CH_3+M = C_2H_6+M$ | $1.27 \cdot 10^{41}$ | −7.0 | 2762 | [21] |
| 7 | $C_2H_6+CH_3 = C_2H_5+CH_4$ | $2.0 \cdot 10^{13}$ | 0.0 | 13,513 | [25] |
| 8 | $C_2H_6+H = C_2H_5+H_2$ | $1.44 \cdot 10^{9}$ | 1.5 | 7412 | [24] |
| 9 | $C_2H_6+M = C_2H_5+H+M$ | $6.63 \cdot 10^{48}$ | −8.24 | 93,577 | [24] |
| 10 | $C_2H_5+M = C_2H_4+H+M$ | $1.0 \cdot 10^{17}$ | 0.0 | 31,072 | [21] |
| 11 | $C_2H_4+CH_3 = C_2H_3+CH_4$ | $4.16 \cdot 10^{12}$ | 0.0 | 11,128 | [26] |
| 12 | $C_2H_4+M = C_2H_3+H+M$ | $2.60 \cdot 10^{17}$ | 0.0 | 96,200 | [21] |
| 13 | $C_2H_4+H = C_2H_3+H_2$ | $5.42 \cdot 10^{14}$ | 0.0 | 14,904 | [24] |
| 14 | $C_2H_3+M = C_2H_2+H+M$ | $4.16 \cdot 10^{41}$ | −7.5 | 45,507 | [21] |
| 15 | $C_2H_2+C_2H_2 = i\text{-}C_4H_3+M$ | $6.31 \cdot 10^{13}$ | 0.0 | 41,600 | [21] |
| 16 | $n\text{-}C_3H_7 = C_3H_6+H$ | $1.0 \cdot 10^{14}$ | 0.0 | 37,286 | [27] |
| 17 | $n\text{-}C_3H_7 = C_2H_4+CH_3$ | $1.20 \cdot 10^{13}$ | 0.0 | 30,303 | [26] |
| 18 | $C_3H_6 = C_2H_3+CH_3$ | $6.31 \cdot 10^{15}$ | 0.0 | 85,800 | [28] |
| 19 | $i\text{-}C_4H_3+H = C_4H_2+H_2$ | $5.0 \cdot 10^{13}$ | 0.0 | 0 | [29] |
| 20 | $i\text{-}C_4H_3+M = C_4H_2+H+M$ | $4.46 \cdot 10^{15}$ | 0.0 | 46,516 | [30] |
| 21 | $AB+e \rightarrow A + B + e$,<br>$[AB] > 10^{-2}$ | See text | | | |
| 22 | $HCO+M = H+CO+M$ | $1.56 \cdot 10^{14}$ | 0.0 | 15,700 | [24] |
| 23 | $HCO+O_2 = HO_2+CO$ | $1.20 \cdot 10^{10}$ | 0.807 | −727 | [31] |
| 24 | $CH_2O+CH_3 = HCO+CH_4$ | $7.80 \cdot 10^{8}$ | 6.1 | 1970 | [24] |
| 25 | $CH_3O+M = CH_2O+H+M$ | $5.40 \cdot 10^{13}$ | 0.0 | 13,500 | [24] |
| 26 | $C_2H_3+O_2 = HCO+CH_2O$ | $5.42 \cdot 10^{12}$ | 0.0 | 0 | [21] |
| 27 | $2OH+M = H_2O_2+M$ | $2.90 \cdot 10^{17}$ | −0.76 | 0 | [21] |
| 28 | $CH_3+H_2O_2 = HO_2+CH_4$ | $1.21 \cdot 10^{10}$ | 0.0 | 596 | [32] |
| 29 | $CH_3+O_2 = OH+CH_2O$ | $3.40 \cdot 10^{11}$ | 0.0 | 8940 | [21] |
| 30 | $H+O_2 = OH+O$ | $9.75 \cdot 10^{13}$ | 0.0 | 14,852 | [33] |
| 31 | $HO_2+CH_3 = O_2+CH_4$ | $3.61 \cdot 10^{12}$ | 0.0 | 0 | [32] |
| 32 | $CH_3+O_2 = CH_3O+O$ | $1.32 \cdot 10^{14}$ | 0.0 | 31,398 | [13] |

the time of streamer propagation is several microseconds, while the times of the chemical processes are several orders of magnitude larger, and consequently, they can be considered independently of one another.

The kinetic mechanism used in the work was constructed of several detailed kinetic models of methane oxidation [16, 17] by selecting reactions on the basis of an analysis of the contribution of each reaction to the decomposition of methane. The abbreviated mechanism involves 31 gas reactions with the participation of 23

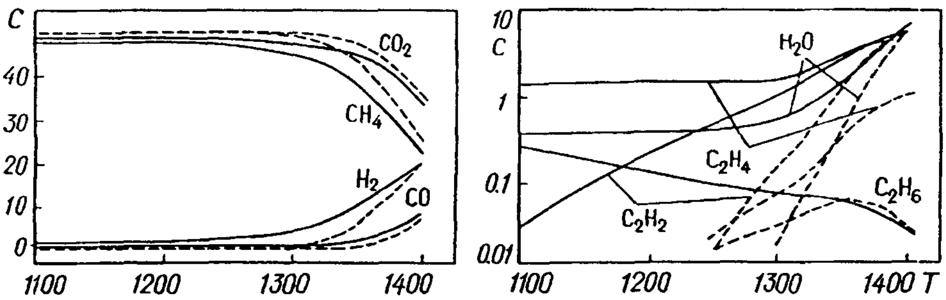

Fig. 2. Effect of the gas temperature on the yield of the products of methane decomposition in a gaseous mixture of $CH_4/CO_2$ = 50:50. The solid lines denote the action of a 10-W gas dischage on the gaseous mixture, and the dashed lines denote thermal decomposition of the gas. C, %; T, K.

components. The reactions used are enumerated in Table 1. The rate constants for the inverse processes were calculated based on thermodynamic data taken from [17]. The participation of ions was disregarded in the work since the concentration of the latter is low compared to the electron concentration under the given conditions [18]. Oxidation processes were described by reactions 22–31.

The primary products of electron-impact dissociation of methane are $CH_3$, $CH_2$, and CH radicals. The most significant contribution to subsequent conversion of the products of methane decomposition is made by the reactions with $CH_3$ radicals, and therefore, in what follows, we did not consider the reactions with CH and $CH_2$ radicals. In addition to the dissociation of methane molecules, we also allowed for electron-impact dissociation of all molecules whose relative concentration exceeded a value of $10^{-2}$. The change in the molecular concentration of the gaseous mixture with time under isothermal conditions was calculated using a standard program for solving equations of chemical kinetics by the Gear method for rigid systems of differential equations [19].

The gaseous-mixture temperature is the most important parameter that characterizes the process of methane decomposition. Figure 2 gives the concentrations of the principal components as functions of the gas temperature. The calculations were performed for a mixture of $CH_4/CO_2$ = 50/50 at atmospheric pressure, a gas-flow velocity of 40 $cm^3$/sec, and a supplied power of 10 W. As shown in the figure, less than 2% of the molecules of the initial mixture decompose at temperatures lower than 1200 K. The degree of conversion under these conditions is practically independent of the gas temperature and is determined only by the magnitude of the supplied power. The molecules of the gaseous medium are transformed by dissociation of them by electron impact. The principal reactions are reactions 21, 1–3, and 6 of Table 1, while the principal products are $H_2$, $CO_2$, ethane, and water. An increase in the gas temperature leads to an increase in the degree of methane conversion. This can be explained by growth of the contribution of the reactions having high activation energies (see Table 1). At temperatures above 1200 K, it is the contribution of the reactions involving radicals that become substantial along with the processes of electron-impact dissociation. As our calculations show, the reactions with H radicals (reactions 1 and 5 in Table 1) are the principal channels of "destruction" of $CH_4$ and $CO_2$ molecules. The principal channels of methane decomposition under the given conditions are shown schematically in Fig. 3. The intensity of the processes is illustrated by the thickness of the lines. According to this scheme, $CH_3$ radicals appear in decomposition reactions 1–3 and in dissociation of methane by electron impact. Associative-recombination reaction 6 of Table 1 leads to formation of ethane molecules ($C_2H_6$), which break down into $C_2H_5$ radicals in reactions 7 and 8 with the H and $CH_3$ radicals. Decomposition of $C_2H_5$ (reaction 10 in Table 1) leads to the appearance of ethylene molecules ($C_2H_4$), which in turn form $C_2H_3$ radicals in reactions 11 and 13. An alternative channel is production of an $n$-$C_3H_7$ radical with subsequent unimolecular disintegration into a $C_3H_6$ molecule (propane) in reactions 16–18. However this reaction is less efficient than the process of ethylene formation. The interaction of $C_2H_4$ molecules with $C_2H_3$ radicals leads to the formation of acetylene molecules ($C_2H_2$), which is described by reaction 14 of Table 1. $C_2H_2$ molecules are partially transformed to an $i$-$C_4H_3$ isomer and can also serve as a source of carbon-black particles; however because of its complexity this process is not considered in the present investigation.

The principal reactions that characterize formation of $H_2$ molecules are decomposition reactions 10, 14, and 16 (the dashed lines in Fig. 3), whose contribution increases with temperature. As Table 1 shows, the activation

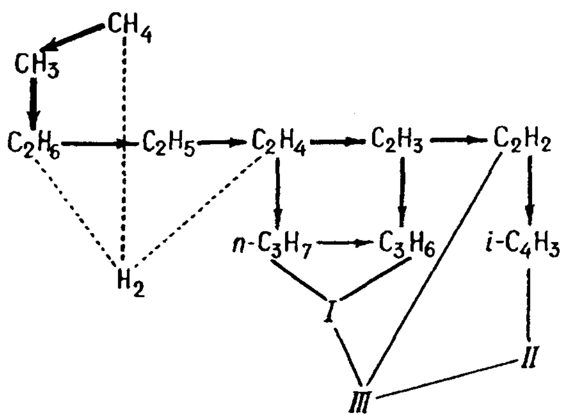

Fig. 3. Principal channels of methane decomposition in a gas discharge: I) aromatic molecules; II) polyene molecules; III) carbon-black particles.

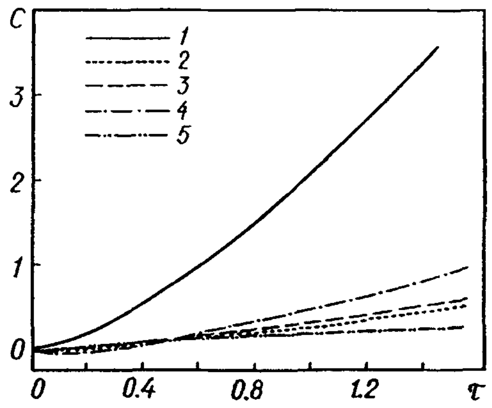

Fig. 4. Time evolution of the principal components of a gaseous mixture of $CH_4/CO_2 = 50:50$ ($P = 1$ atm, $T = 1300$ K): 1) $H_2$; 2) $H_2O$; 3) CO; 4) $C_2H_2$; 5) $C_2H_4$. $\tau$, sec.

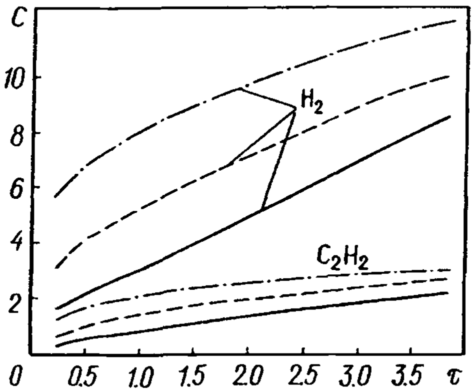

Fig. 5. Effect of the lifetime of particles in a reactor on the formation of the main products of methane decomposition. The solid lines are a power of 10 W, the dashed lines are a power of 20 W, and the dot-dash lines are a power of 40 W ($T = 1300$ K).

energies of these reactions are comparatively low, and therefore the latter predominate under the conditions considered.

Unlike $CH_4$, decomposition of carbon dioxide molecules is not efficient under the conditions described. This is a difference of a conversion process in a gas discharge from a catalytic process in which both $CO_2$ and $CH_4$ molecules take an active part in decomposition reactions. As our calculations show, the contribution of reaction 5 (see Table 1), in which $CO_2$ molecules participate with H radicals, is the most substantial. As a result of this reaction, molecules of carbon dioxide are destroyed, their degree of conversion being much lower than the degree of conversion of methane molecules under the same conditions, as shown in Fig. 2. The low efficiency of the processes involving $CO_2$ causes a comparatively low concentration of molecules of CO and water as compared to the yield of molecular hydrogen and hydrocarbons.

Methane conversion is enhanced substantially with increase in the lifetime of molecules of the medium in the reactor. Figure 4 shows the time evolution of mixture molecules for the same conditions as in Fig. 2. As can be seen from Fig. 4, the yield of the products increases in proportion to $\tau$, which demonstrates the absence of saturation. To allow for the effect of the particle lifetime on methane conversion, we introduced a damping factor for the dissociation frequency that makes it possible to avoid the distortion of the applied electric field. Results of calculating the concentration of the products of methane decomposition as a function of the applied power of the electric field are shown in Fig. 5. The calculation was performed for the same conditions as in Fig. 4. The product

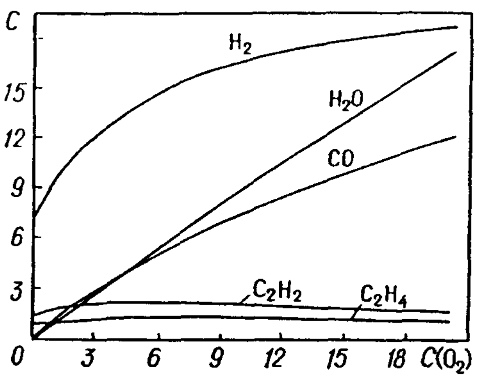

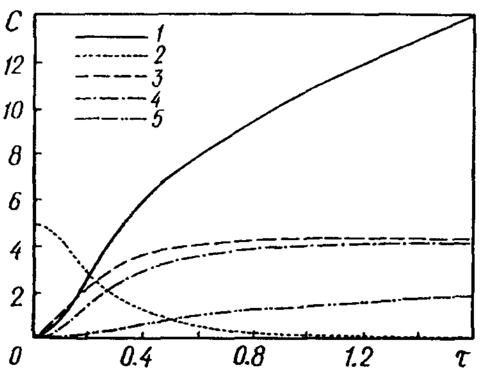

Fig. 6. Effect of the initial concentration of oxygen on the yield of products of methane decomposition ($T = 1300$ K). $C(O_2)$, %.

Fig. 7. Time evolution of components of a mixture of $CH_4/O_2 = 95{:}5$ ($T = 1300$ K): 1) $H_2$, 2) $O_2$, 3) $H_2O$, 4) CO, 5) $C_2H_2$.

yield increases with the particle lifetime; no saturation effect is observed. With increase in $\tau$ above 5 sec no substantial change in the degree of methane conversion occurs. This can be explained by the increase in the contribution of thermal dissociation, which becomes comparable to or exceeds the efficiency of electron-impact dissociation. The degree of conversion is increased by increasing the supplied power. As a comparison of the curves in Fig. 5 shows, the growth in the concentration of the main products of methane decomposition is practically proportional to the power. To characterize the energy consumption, we should note that a supplied power of 40 W for times of the order of 1.6 sec corresponds to 35% of the total heat energy required for heating the gaseous mixture to a temperature of 1300 K.

Adding water in catalytic transformation of $CH_4$ at high pressure leads to a substantial increase in the degree of methane conversion [20]. Reactions between water molecules and hydrocarbons are highly endothermic, as is known, and therefore they occur in the presence of a catalyst or under conditions of elevated temperatures. We investigated the process of decomposition of a $CH_4/H_2O$ mixture under gas-discharge conditions, and we observed no pronounced effect of small water additions (of the order of 5–10%) on the hydrogen yield under these conditions. Nonetheless, a small addition of water can prove important for the following reason. It is known that methane decomposition in a gas-discharge plasma is accompanied by formation of carbon-black particles. Their concentration is rather high and leads to deposition of carbon black on the reactor walls, particularly under conditions of high temperatures. A small addition of water to the gaseous mixture can decrease substantially the yield of carbon-black particles without decreasing the degree of methane conversion. Unlike water, adding oxygen to the gaseous mixture leads to significant acceleration of methane decomposition. The effect of the initial oxygen concentration on the yield of the main products of methane decomposition is shown in Fig. 6. The calculation was performed for the same conditions as in Fig. 2; a difference was observed only in the composition of the initial mixture. Even a small amount of oxygen molecules leads to an increase in the hydrogen yield, whose optimum value is attained with a 5% initial concentration of $O_2$. As the oxygen concentration in the mixture increases further, the concentration of $H_2O$ molecules increases while the efficiency of the yield of CO and hydrocarbon molecules decreases. The time evolution of the principal components of a mixture of $CH_4/O_2 = 95/5$ is given in Fig. 7. As a comparison of Figs. 4 and 7 shows, the time distribution of the mixture products differs substantially from that observed in $CH_4/CO_2$ mixtures. The process of methane decomposition in oxygen mixtures can be represented in the form of two steps. The first step is characterized by high concentrations of O and OH radicals and efficient formation of $H_2$ molecules. In the second step, which corresponds to times larger than 0.5 sec, oxygen molecules are "destroyed," the concentration of the radicals decreases, and methane decomposition proceeds by the mechanism presented in Fig. 3.

Thus, in the work, we showed the possibility of intense methane decomposition in different mixtures in a gas discharge. The most efficient conversion of methane is observed under the action of a gas discharge on a gaseous mixture preheated to a temperature of 1200 K, for which thermal dissociation of methane is insignificant. The degree of methane conversion under these conditions exceeds the value obtained in simple heating of the gas to a temperature of 1400 K (see Fig. 3). It can be inferred that a rather high yield of hydrogen molecules within the framework of our model (15–20%) is observed at comparatively low temperatures (1200–1300 K). An increase in the molecular lifetime to 1.6 sec and small oxygen additions to the initial gaseous mixture are capable of increasing significantly the yield of the products of methane decomposition. The optimum yield of molecular hydrogen is attained with a 5% initial concentration of $O_2$ and amounts to 14% at a temperature of 1300 K and atmospheric pressure.

## NOTATION

$T$, temperature, K; $\tau$, lifetime of the molecules, sec; $E/N$, reduced electric field, $V \cdot cm^2$; $\nu^{diss}$, dissociation frequency, $sec^{-1}$; $E$, electric-field strength, V/cm; $N$, concentration of neutral particles, $cm^{-3}$; $N_e$, local concentration of electrons, $cm^{-3}$; $Q$, fraction of the electric-field energy, %; $C$, concentration, %; $C(O_2)$, concentration of $O_2$ molecules, %; $k$, rate constant for the chemical reaction, $cm^3/sec$; $k = A \cdot T^n \exp(-E_a/T)$; $A$, preexponential factor, $cm^3/(mole \cdot sec)$; $n$, exponent; $E_a$, activation energy, cal·mole; $\langle u \rangle$, average energy of the electrons, eV. Superscript and subscript: diss, dissociation; a, activation.

## REFERENCES

1. M. G. Poirier and C. Sapundzhiev, Int. J. Hydrogen Energy, 22, 429-434 (1997).
2. G. Nicoletti, Int. J. Hydrogen Energy, 20, 759-765 (1995).
3. M. A. Rosen, Int. J. Hydrogen Energy, 21, 349-355 (1996).
4. H. Gladish, Hydrocarbon Processing & Petroleum Refiner, 41, 159-161 (1962).
5. R. J. Tedeschi, Acetylene-Based Chemicals from Coal and Other Natural Resources, New York (1982).
6. H. Nassar, K. Meguernes, A. Csernichowski, and J. Chappelle, Proc. of 12th Int. Symp. Plasma Chemistry, Aug. 21-25, 1995, Minneapolis (1995), pp. 651-653.
7. S. Masuda and H. Nakao, IEEE Trans. Industry Appl., 26, 374-380 (1990).
8. L. G. H. Huxley and R. W. Crompton, The Diffusion and Drift of Electrons in Gases, New York (1974).
9. H. F. Winters, J. Chem. Phys., 63, 3465-3472 (1975).
10. M. Hayashi, in: Swarm Studies and Inelastic Electron-Molecule Collisions (eds. L. C. Pitchford, B. V. McKoy, A. Chutzian, and S. Trajmar), New York (1987), p. 167.
11. J. Lowke, Appl. Phys., 43 4664-4670 (1973).
12. P. I. Porshnev, Inzh.-Fiz. Zh., 58, No. 5, 814-819 (1990).
13. P. I. Porshnev, O. V. Petrova, and S. A. Zhdanok, Report on Research and Development Services Agreement of November 1, 1995, R&D Enterprise "Chemical Physics Technologies," Minsk (1995), pp. 5-65.
14. S. A. Lawton and A. V. Phelps, J. Chem. Phys., 69, 1055-1065 (1978).
15. G. S. P. Castle, I. I. Inculet, and K. I. Burgess, IEEE Trans. Ind. and Gen. Appl., IGA-5, 489-496 (1969).
16. C. T. Bowman, R. K. Hanson, D. F. Davidson, W. C. Gardiner, Jr., V. Lissianski, G. P. Smith, D. M. Golden, M. Frenklach, and M. Goldenberg, GRI-Mech, Version 2.11. 11/3/95. 1st release 9/6/95. 1995. http://www.me.berkeley.edu/gri.mech.
17. A. A. Konnov, Detailed Reaction Mechanism for Small Hydrocarbons Combustion, Release 0.21. 1997. 27th Int. Symp. on Combustion. http://homepages.vub.ac.be/-akonnov/.
18. J. J. Lowke and R. Morrow, Proc. of 12th Int. Symp. Plasma Chemistry, Aug. 21-25, 1995, Minneapolis (1995), pp. 1813-1815.
19. O. V. Petrova, A. P. Chernukho, P. I. Porshnev, and S. A. Zhdanok, Inzh.-Fiz. Zh., 71, No. 2, 299-305 (1998).
20. K. E. Cox and K. D. Williamson, Hydrogen: Its Technology and Implications, Vol. 1 (1997).
21. D. L. Baulch, C. J. Cobos, R. A. Cox, C. Esser, P. Frank, Th. Just, J. A. Kerr, M. J. Pilling, J. Troe, R. W. Walker, and J. Warnatz, J. Phys. Chem. Ref. Data, 21, 411-417 (1977).
22. J. W. Sutherland and J. Michael, J. Phys. Chem., 90, 5941-5950 (1986).

23. C. J. Cobos and J. Z. Troe, Phys. Chem. (Neue Folge), 167, 129-135 (1990).
24. D. L. Baulch, C. J. Cobos, R. A. Cox, P. Frank, G. Hayman, Th. Just, J. A. Kerr, T. Murrells, M. J. Pilling, J. Troe, R. W. Walker, and J. Warnatz, J. Phys. Chem. Ref. Data, 23, 847-860 (1994).
25. W. Moller, E. Mozzhukhin, and H. Gg. Wagner, Ber. Bunsenges. Phys. Chem., 91, 660-669 (1987).
26. J. Warnatz, in: Rate Coefficients in the C/H/O System (ed. W. C. Gardiner, Jr.), New York (1984), p. 197.
27. R. P. Duran, V. T. Amorebieta, and A. J. Colussi, J. Phys. Chem., 92, 636-640 (1988).
28. W. Tsang, J. Phys. Chem. Ref. Data, 17, 887-895 (1988).
29. Y. Tan, Ph. Dagaut, M. Cathonnet, and J. C. Boettner, Combust. Sci. and Technol., 102, 21-26 (1994).
30. J. A. Miller and C. F. Melius, Combust. Flame, 91, 21-28 (1992).
31. C.-C. Hsu, A. M. Mebel, and M. C. Lin, J. Chem. Phys., 105, 2346-2356 (1996).
32. W. Tsang and R. F. Hampson, J. Phys. Chem. Ref. Data, 15, 1087-1093 (1986).
33. H. Du and J. P. Hessler, J. Chem. Phys., 96, 1077-1092 (1992).